

Efficient in-depth trapping with an oil-immersion objective lens

S. Nader S. Reihani, Mohammad A. Charsooghi, Hamid R. Khalesifard, and Ramin Golestanian

Institute for Advanced Studies in Basic Sciences, Gava Zang, Zanjan 45195-1159, Iran

Received September 12, 2005; revised November 29, 2005; accepted December 8, 2005; posted December 12, 2005 (Doc. ID 64759)

Maximum trapping efficiency in optical tweezers occurs close to the coverslip because spherical aberration owing to a mismatch in the refractive indices of the specimen (water) and the immersion oil dramatically decreases the trap efficiency as the trap depth increases. Measuring the axial trap efficiency at various tube lengths by use of an oil-immersion objective has shown that such an aberration can be balanced by another source of spherical aberration, leading to a shift in the position of the maximum efficiency in the Z direction. For a $1.1\text{ }\mu\text{m}$ polystyrene bead we could achieve the maximal efficiency at a depth of $70\text{ }\mu\text{m}$, whereas the trap was stable up to a depth of $100\text{ }\mu\text{m}$. © 2006 Optical Society of America

OCIS codes: 140.7010, 120.4570.

Optical trapping by focusing a laser beam with a high-numerical-aperture lens has recently attracted much attention and is widely used in various applications.^{1–3} A common problem with using the oil-immersion objective lenses in optical tweezers (and in confocal microscopy as well) is the presence of optical aberrations, especially spherical aberrations, which cause poor trapping performance. The design of the objective lenses is such that the spherical aberration that arises from a mismatch in the refractive indices of immersion oil and the specimen is compensated for at depths of the order of a few micrometers (compensated depth). For deeper focusing, the spherical aberration is dramatically increased, causing a poorer trapping efficiency. Using water-immersion objective lenses could be a solution for trapping at greater depths because of the small contrast of the refractive indices. However, such objective lenses typically have low numerical apertures: Although theoretically the numerical apertures of such lenses can reach 1.33, the highest available numerical aperture is ~ 1.2 . Oil-immersion objectives can have considerably higher numerical apertures; a numerical aperture of 1.65 is available now.

A more practical way to compensate for aberrations could be to try to reposition the compensated depth by introducing an additional source of spherical aberration with opposite sign. Changing the tube length has been suggested,^{4,5} and investigated in the lateral direction.⁶ Previous studies have shown improvement in efficiency toward partial compensation as the tube length is changed,^{4–6} although complete compensation away from the surface was not achieved. In this Letter we report measurements of the axial trapping efficiency with oil-immersion objectives corrected for finite and infinite distance and show that full compensation can be achieved at an arbitrary depth in the chamber by tuning the tube length as a parameter.

Our optical tweezer setup (Fig. 1) is based on a custom-designed inverted microscope.⁶ The microscope is designed for transillumination, bright field, finite, and infinite tube-length imaging of the sample with simultaneous use of a laser source ($1.064\text{ }\mu\text{m}$; Model Compass/2000, Coherent) as an optical twee-

zer. Lenses L1 and L2 were used to collimate the beam to a diameter of 5 mm. Figure 1 shows the system in the standard finite-tube-length (160 mm) mode. The objective was mounted upon a piezo-equipped objective holder (P-723.10 objective positioner; Physik Instrumente).

Tube length is defined as the distance from the back focal plane (BFP) of the objective to the focus of the laser [Fig. 2(a)]. The position and the focal length of lens Lt define the tube length. In the finite tube-length mode the diverging beam hits the BFP of the objective, whereas in the infinite-tube-length mode the laser beam was collimated to a diameter of 10 mm before the objective by introduction of an extra lens [Fig. 2(b)] and the parallel beam rays hit the BFP of the objective. We introduce a third case as the *negative* tube length at which a converging laser beam hits the BFP of the objective [Fig. 2(c)]. As in the first case the magnitude of the tube length is defined as the distance between the BFP of the objective and the virtual focal point of the laser, and it can be controlled by the position and the focal length of lens Lnt. Note that here it is necessary to expand the

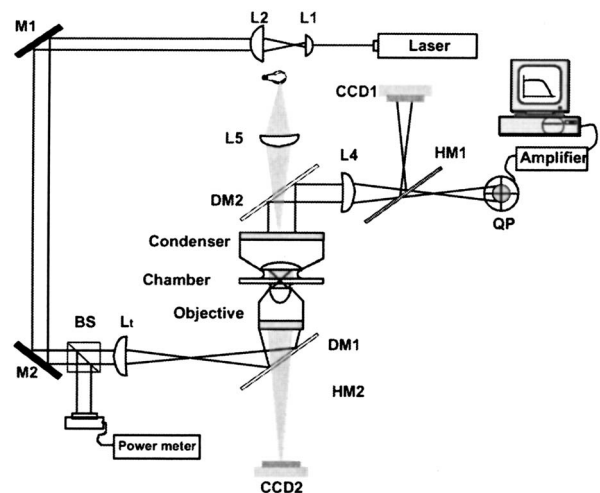


Fig. 1. Schematic of the optical tweezer: L1, L2, L4, L5, Lt, lenses; BS, beam splitter; M1, M2, mirrors; HM1, HM2, half-mirrors; DM1, DM2, dichroic mirrors; CCD1, CCD2, charge-coupled devices; QP, quadrant photodiode.

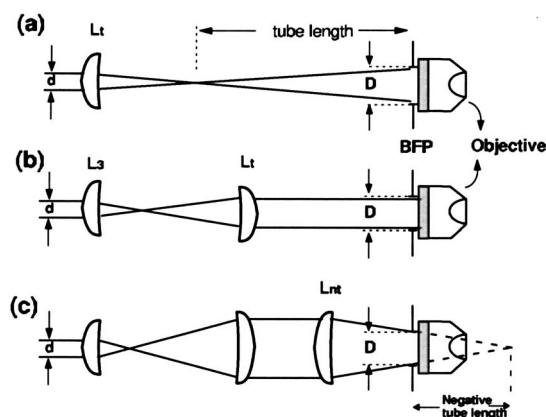


Fig. 2. Schematics of (a) finite, (b) infinite, and (c) negative tube lengths.

beam more to overfill the BFP of the objective properly. During the experiment the laser beam was expanded to a diameter of 20 mm before focusing by lens Lnt.

To show how variation in tube length can compensate for spherical aberration we measured the axial trapping efficiency by using the escape force method—with tube length as a parameter—for 1.1 μm latex beads (LB-11; Sigma) mixed in to double-distilled water. The objective was moved back and forth with an amplitude of 5 μm at various velocities with respect to the stationary chamber while a bead was in the trap. As the amplitude of movements is much smaller than the tube lengths (less than 0.05%), changes in input laser power can be neglected. For each tube length the escape velocity (the velocity at which a bead escapes the trap) was measured at various depths. Note that the bead is far enough from the glass's surface that no correction term is necessary for conformity to Stokes law.⁷ Figure 3(a) shows the results for a finite-distance-corrected achromat objective (effective aperture EA 100 \times , 160 mm tube length, 1.25 NA; Olympus).

Table 1 lists the focal lengths and the positions (with respect to the BFP of the objective) of lens Lt [Fig. 1] that were used to produce the first five tube lengths in Fig. 3(a). A simple ray optics calculation will show that all the cases in Table 1 will produce a beam diameter of 10 mm at the BFP of the objective. For a tube with infinite length, two telescopic lenses were used [Fig. 2(b)]. The focal lengths of the lenses were 15 and 30 cm to double the beam diameter (10 mm). For negative tube length, first the beam was expanded four times (diameter of 20 mm) and then a long-focal-length converging lens was positioned at a distance equal to half of its focal length upstream of the objective such that the beam diameter at the BFP of the objective was 10 mm, as in the other cases. To make the CCD2 parfocal with the tweezers, we mounted it upon a linear positioner, and an imaging lens was used in front of CCD2. We then used CCD2 to get a focused image of the bead in the trap at each tube length. We used the glass surface as a reference with which to measure the depth, and we used the common method of video microscopy to find the surface, as follows: A bead was trapped and was pushed

against the surface. Once it touched the surface, it was pushed out of focus in the CCD screen, hence defining the depth.

The method described above was useful for the first three tube lengths, but for the others it was not possible to keep the bead in a trap in the vicinity of the glass surface. For the rest of the tube lengths in Fig. 3, the depth of the maximum escape velocity was used as a reference point as follows: The bead in the trap at the depth of the maximum escape velocity was brought into focus; then the objective was moved to yield a sharp image from a bead stuck to the glass surface. The magnitude of such a movement was considered the depth of the maximum escape velocity.

The results for the escape velocity of the bead as a function of the focusing depth presented in Fig. 3 are interesting in that the data develop peaks at certain optimized depths that correspond to the compensation for the spherical aberration. Moreover, the peak in Fig. 3(a) becomes systematically deeper as the tube length is increased toward infinity. This process

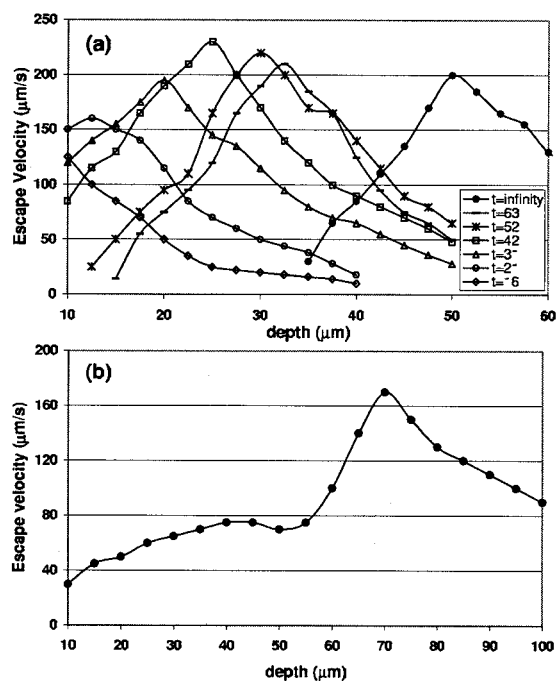


Fig. 3. Escape velocity versus trapping depth with tube length as a parameter for a finite-distance-corrected objective lens: (a) positive and infinite tube lengths (in centimeters), (b) typical negative tube length ($t = -25$ cm). The laser power was 23.6 mW before the objective.

Table 1. Focal Lengths and Positions with Respect to the BFP of the Objective of the Lenses that Were Used to Produce the Tube Lengths

Tube Length (cm)	Focal Length (cm)	Position (cm)
16	8	24
21	10	31
31	15	46
42	20	62
53	25	78
63	30	93

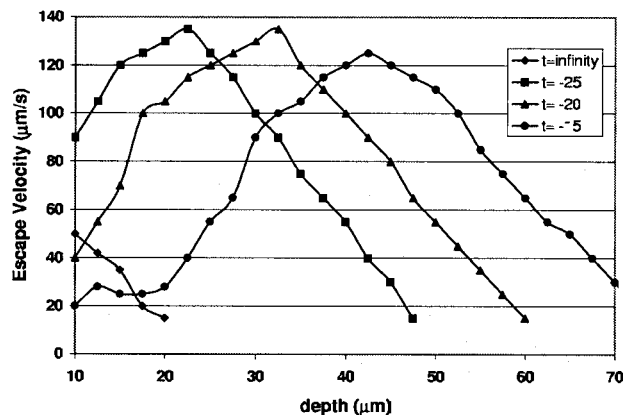


Fig. 4. Escape velocity versus trapping depth with tube length (in centimeters) as a parameter for an infinite-distance-corrected objective lens. The laser power was 23.6 mW before the objective.

could be continued further by use of negative tube lengths [defined in Fig. 2(c)]. An example of this case is presented in Fig. 3(b) for $t = -25$ cm, which develops the compensated depth at $70 \mu\text{m}$. Note that in this case the trap was stable up to a depth of $100 \mu\text{m}$.

We repeated the experiment for an infinity-corrected achromat lens ($100\times$, ∞ , 1.25 NA; Zeiss), the result of which is shown in Fig. 4. We observed that only the negative tube lengths could help to shift the maximum efficiency depth. Three negative tube lengths were investigated. Note that the compensated depths shift to the right as tube length t becomes a smaller negative number. It is worth mentioning that the magnitudes of the maximum escape velocity illustrated in Figs. 3 and 4 are considerably higher than the typical values obtained in conventional optical tweezers.

Spherical aberration could degrade the Gaussian shape of the intensity profile at the beam waist—it decreases the strength of the central peak and increases the strength of the sidelobes in the intensity profile—which reduces the imaging resolution in confocal microscopy.⁴ As the gradient of the intensity profile at the focal plane defines the stiffness (and the efficiency) of the trap, this means that the peak in each of the traces in Figs. 3 and 4 indicates the depth at which the intensity profile has the sharpest shape. Such sharpening of the beam profile can be used in confocal microscopy to increase the resolution of imaging for thick specimens.

In conclusion, we have shown that tube length can be used as a suitable parameter with which to tune optical tweezers into the optimal condition at which spherical aberration is compensated for at a given depth. The present technique provides the ability to trap small particles far deeper in the chamber than can be achieved by conventional optical tweezers. For example, a $1.1 \mu\text{m}$ latex bead can normally be stably trapped up to the depth of $\sim 20 \mu\text{m}$,⁸ whereas with the method described here we can achieve a strong trap up to a depth of $\sim 100 \mu\text{m}$. This depth could be increased even further when so-called long-working-distance objective lenses were used.⁹ Such an ability could be important for experiments that should be done far from the chamber walls. Our data suggest that finite-distance-corrected objectives are in fact more suitable for such a shift in compensation depth, because they provide a wider range of change in the tube length and a bigger contrast in efficiency, which could be used in designing tunable robust traps far away from the glass surface.

S. N. S. Reihani's e-mail address is reihani@iasbs.ac.ir.

References

1. C. Bustamante, Z. Bryant, and S. B. Smith, *Nature* **421**, 423 (2003).
2. K. Svoboda, C. F. Schmidt, B. J. Schnapp, and S. M. Block, *Nature* **365**, 721 (1993).
3. A. Ashkin, J. M. Dziedzic, J. E. Bjorkholm, and S. Chu, *Opt. Lett.* **11**, 288 (1986).
4. C. J. R. Sheppard, M. Gu, K. Brain, and H. Zhou, *Appl. Opt.* **33**, 616 (1994).
5. P. C. Ke and M. Gu, *J. Mod. Opt.* **45**, 2159 (1998).
6. S. N. S. Reihani, H. R. Khalesifard, and R. Golestanian, *Opt. Commun.* **259**, 204 (2006).
7. B. Lin, J. Yu, and S. A. Rice, *Phys. Rev. E* **62**, 3909 (2000).
8. K. C. Neuman and S. M. Block, *Rev. Sci. Instrum.* **75**, 2787 (2004).
9. The working distance for an objective lens is defined as the distance between the specimen and the front surface of the objective lens. Whereas a typical value of this parameter for a normal objective is $\sim 100 \mu\text{m}$, for long-working-distance objective lenses it could be more than $200 \mu\text{m}$.